Title

Identification of the ZPC oligosaccharide ligand involved in sperm binding and the glycan structures of Xenopus laevis vitelline envelope glycoproteins

Journal

Biology of Reproduction, 69(6)

ISSN

0006-3363

Authors

Vo, L H
Yen, T Y
Macher, B A
et al.

Publication Date

2003-12-01

Peer reviewed

BIOLOGY OF REPRODUCTION **69,** 1822–1830 (2003)
Published online before print 6 August 2003.
DOI 10.1095/biolreprod.103.015370

Identification of the ZPC Oligosaccharide Ligand Involved in Sperm Binding and the Glycan Structures of *Xenopus laevis* Vitelline Envelope Glycoproteins[1]

Loc H. Vo,[3] Ten-Yang Yen,[4] Bruce A. Macher,[4] and Jerry L. Hedrick[2,3]

Section of Molecular and Cellular Biology,[3] University of California, Davis, California 95616
Department of Chemistry and Biochemistry,[4] California State University, San Francisco, California 94132

ABSTRACT

The *Xenopus laevis* egg vitelline envelope is composed of five glycoproteins (ZPA, ZPB, ZPC, ZPD, and ZPX). As shown previously, ZPC is the primary ligand for sperm binding to the egg envelope, and this binding involves the oligosaccharide moieties of the glycoprotein (*Biol. Reprod.,* 62:766–774, 2000). To understand the molecular mechanism of sperm-egg envelope binding, we characterized the *N*-linked glycans of the vitelline envelope (VE) glycoproteins. The *N*-linked glycans of the VE were composed predominantly of a heterogeneous mixture of high-mannose (5-9) and neutral, complex oligosaccharides primarily derived from ZPC (the dominant glycoprotein). However, the ZPA *N*-linked glycans were composed of acidic-complex and high-mannose oligosaccharides, ZPX had only high-mannose oligosaccharides, and ZPB lacked *N*-linked oligosaccharides. The consensus sequence for *N*-linked glycosylation at the evolutionarily conserved residue N^{113} of the ZPC protein sequence was glycosylated solely with high-mannose oligosaccharides. This conserved glycosylation site may be of importance to the three-dimensional structure of the ZPC glycoproteins. One of the complex oligosaccharides of ZPC possessed terminal β-*N*-acetyl-glucosamine residues. The same ZPC oligosaccharide species isolated from the activated egg envelopes lacked terminal β-*N*-acetyl-glucosamine residues. We previously showed that the cortical granules contain β-*N*-acetyl-glucosaminidase (*J. Exp. Zool.,* 235:335–340, 1985). We propose that an alteration in the oligosaccharide structure of ZPC by glucosaminidase released from the cortical granule reaction is responsible for the loss of sperm binding ligand activity at fertilization.

fertilization, gamete biology, ovum, sperm

INTRODUCTION

An extracellular matrix composed of a family of conserved glycoproteins surrounds animal eggs. This matrix, termed the zona pellucida (ZP) or vitelline envelope (VE), functions in fertilization in sperm-egg binding, induction of the sperm acrosome reaction, enzyme-assisted sperm penetration of the envelope, and prevention of polyspermy. In mammals, ZP glycoproteins are derived from three conserved gene families [1] that are evolutionarily conserved from fish to mammals [2]. These glycoproteins (ZPA, ZPB, and ZPC) are expressed during oocyte maturation and assembled into a three-dimensional matrix around the egg. Sperm interactions with the VE/ZP involve receptors on the plasma membrane surface that recognize and bind oligosaccharide ligands of the envelope glycoproteins.

Carbohydrate recognition is generally recognized as playing a critical role in sperm-egg envelope interactions. In the mouse, *O*-linked oligosaccharides of ZPC glycoproteins were proposed as the ligands for sperm adhesion and an inducer of the acrosome reaction [3, 4]. In the pig, both *N*-linked and *O*-linked oligosaccharides have been proposed to be involved in sperm binding [5, 6]. Furthermore, sperm binding in the pig has been proposed to be dependent on the hetero-oligomeric interaction of ZPC and ZPB [7]. In bovine gamete interaction, sperm binding to the ZP involves *N*-linked oligosaccharides [8]. Sperm binding in anurans has been attributed to the ZPC component of the VE for both *Xenopus laevis* and *Bufo japonicus* [9, 10]. In both these studies involving *Xenopus* and *Bufo*, sperm-VE binding was associated with carbohydrate-protein interactions. However, Tian et al. [11] also reported the significance of carbohydrates in *Xenopus* sperm-VE binding but attributed this interaction to ZPA oligosaccharides. Thus, there is agreement that sperm-envelope/zona binding involves oligosaccharides but a lack of agreement on the specific glycoproteins and oligosaccharides involved.

The *Xenopus* VE is composed of at least five glycoproteins: ZPA (64/69 kDa), ZPB (37 kDa), ZPC (41 kDa), ZPD (80 kDa), and ZPX (112/120 kDa). Based on Coomassie blue staining of SDS-PAGE-separated glycoproteins, the weight percent composition of the VE for ZPA, ZPB, ZPC, and ZPX is 4.5%, 39.3%, 43.3%, and 12.8%, respectively. ZPD is a minor component contributing less than 1% of the VE composition (37). All envelope glycoproteins have been cloned and possess 4 (ZPA), 0 (ZPB), 2 (ZPC), 8 (ZPD), and 14 (ZPAX) potential *N*-linked glycosylation sites, respectively [2, 17–19, 37]. Fucose (Fuc) and GlcNAc residues of *N*-linked oligosaccharides have previously been shown to have essential functions in sperm-VE binding [9].

Although egg envelope oligosaccharide structures for other species are known, no structural information is available for the envelope glycans of *Xenopus* [8, 20, 21]. The present study was undertaken to determine and structurally characterize oligosaccharide ligands that mediate sperm binding in *Xenopus*.

MATERIALS AND METHODS

Sperm, Egg, and Vitelline Envelope Preparation

Investigations were conducted in accordance with the Guiding Principles for the Care and Use of Research Animals. Methods for the procurement of eggs, envelopes, and sperm were essentially those of Hedrick and Hardy [22]. Sperm were counted with a hemocytometer and stored in DeBoers (DB) solution at 4°C until use. The sperm solution was generally diluted to 0.33 DB solution with water immediately before use in the sperm binding assays.

[1]Research was supported in part by NSF research grant MCB 9728447.
[2]Correspondence: Jerry Hedrick, Section of Molecular and Cellular Biology, University of California, One Shields Ave., Davis, CA 95616-8535. FAX: 530 752 3085; e-mail: jlhedrick@ucdavis.edu

Received: 10 January 2003.
First decision: 6 February 2003.
Accepted: 23 June 2003.

ISSN: 0006-3363. http://www.biolreprod.org

Isolation of VE Glycoproteins

VE glycoproteins were isolated by continuous-elution SDS-PAGE using a Bio-Rad 491 Cell Prep (Hercules, CA). Initially, envelopes were solubilized by heating in Laemmli sample preparation buffer at 100°C for 5 min under reducing conditions. Approximately 1 mg of VE was loaded onto the Cell Prep with an 8% gel. Electrophoresis was at 40 A (constant current), and fractions were collected every 3 min with a flow rate of 1 ml/min. The fractions were analyzed with conventional SDS-PAGE and silver staining. Fractions containing similar VE components were pooled, dialyzed, and lyophilized. To further purify the components, the pooled samples were again electrophoretically separated using the Bio-Rad 491 Cell Prep with a 10% gel and the same running conditions as described previously. Fractions containing the same glycoprotein were pooled and dialyzed against water for 48 h. The isolated VE components were stored at −20°C until use.

Hydrazinolysis

VE, ZPC, and ZPB were thoroughly dialyzed and lyophilized before the addition of hydrazine. Hydrazine solutions—200 μl, 50 μl, and 50 μl—were added to 1 mg of VE, 200 μg of ZPC, and 200 μg of ZPB, respectively, and incubated at 60°C for 5 h to release *O*-linked oligosaccharides or 95°C for 4 h to release both *N*-linked and *O*-linked oligosaccharides. Unreacted hydrazine was removed under vacuum. To re-*N*-acetylate the glycans, 500 μl of an ice-cold saturated sodium bicarbonate solution were added to each of the reactions, followed immediately by 125 μl of acetic anhydride. The reaction was incubated for 10 min at room temperature. Another 125 μl of acetic anhydride were added to the reaction and incubated for 20 min. The reaction mixture was then passed through a Dowex AG 50-X12 (H^+) column (Bio-Rad). The column was washed with 5 ml of water. The eluant and washings were combined and rotary evaporated to dryness. Samples were stored at −20°C until use.

Release of N-Linked Oligosaccharides

N-linked oligosaccharides of the VE, VE*, and isolated glycoproteins of the activated and unactivated envelopes were released with PNGase-F (Boehringer Mannheim, Indianapolis, IN). For all glycoprotein samples, a 1:1000 ratio (weight:weight) of PNGase-F:glycoprotein was used and incubated at 37°C for 16 h in a 100-mM ammonium bicarbonate buffer (pH 8.0). Ice-cold ethanol (80% final concentration) was added to each of reaction mixtures to stop hydrolysis and precipitate protein. Reaction mixtures were incubated at −20°C for 30 min and centrifuged at 10 000 × *g* for 5 min at room temperature. The supernate of each digestion mixture, which contained the released glycans, was removed and rotary evaporated to dryness. Samples were stored at −20°C until use. Deglycosylation was monitored by analyzing the pellet of each reaction by SDS-PAGE.

Exo-Glycosidase Treatment of Oligosaccharides

N-linked and *O*-linked oligosaccharides were treated singularly or in combinations with *D. pneumoniae* β-*N*-acetylglucosaminidase (Boehringer Mannheim), bovine kidney β-*N*-acetylhexosaminidase (Boehringer Mannheim), α-mannosidase (Boehringer Mannheim), α-fucosidase (Boehringer Mannheim), and α-galactosidase (Boehringer Mannheim) in a 100-mM ammonium acetate buffer (pH 6.0) for 16 h at 37°C. The equivalent of 0.1 activity unit of the exo-glycosidases was used in all reactions.

Fluorophore Labeling of Oligosaccharides and Electrophoresis

Oligosaccharides, released with peptide *N*-glycosidase F (PNGase F) or hydrazinolysis, were labeled with 8-aminonaphthalene-1,3,6-trisulfonate (ANTS). Dried oligosaccharide samples were derivatized by adding 10 μl of an ANTS solution (0.15 M in 3:17 v/v acetic acid-water solution, Molecular Probes, Eugene, OR) and 10 μl of sodium cyanoborohydride (1.0 M in DMSO). The reactions were incubated at 37°C for 16 h. Reactions were then passed through a TSK-3000-PW column (Phenomenex, Rancho Palos Verdes, CA) to remove contaminants and excess unreacted ANTS. ANTS-labeled oligosaccharide fractions were collected and pooled by fluorescence monitoring using 330-nm excitation and 500-nm emission wavelengths. Fractions were rotary evaporated to dryness. Samples were stored at −20°C until use.

ANTS-labeled oligosaccharides were mixed with 2× load buffer (Glyko, Novato, CA) and were loaded onto either a Fluorophore-Assisted Carbohydrate Electrophoresis (FACE) *N*-linked polyacrylamide gel or FACE *O*-linked polyacrylamide gel (Glyko). An oligosaccharide ladder standard (Glyko) was loaded onto one of the gel lanes. Electrophoresis was at 20 mA for each gel (constant current) with cold running buffer (4°C) for *N*-linked gel electrophoresis and room temperature buffer for *O*-linked gel electrophoresis. Fluorophore-labeled oligosaccharides were visualized with the FACE imaging system (Glyko) with a sensitivity of approximately 10 pmols.

MALDI Mass Spectrometry Analysis of VE Oligosaccharides

The mass analysis for the VE *N*-linked oligosaccharides utilized Fourier transform mass spectrometry (FTMS). Matrix-assisted laser desorption/ionization (MALDI)-FTMS used a commercial instrument (IonSpec Corp., Irvine, CA) with an external MALDI source and a 4.7-T superconducting magnet. Desorption was accomplished by a nitrogen laser (337 nm). Analyzed samples were enriched with cesium or sodium. Samples were concentrated on the probe tip, and 1 μl of 0.4 M 2,5-dihydroxybenzoic acid was added as the matrix.

N-Linked Glycosylation Mapping of ZPC

Isolated ZPC was reduced by the addition of 200-fold molar access of DTT:protein and incubated in 65°C for 30 min. The glycoprotein was then alkylated by adding a 400-fold molar access of iodoacetamide:protein and incubating the reaction at room temperature for 30 min in the absence of light. Isolated ZPC was treated with endoproteinase Lys-C (Boehringer Mannheim) at a ratio of 5:1 (wt:wt) and separated on a C18 column (250 × 4.60 mm; Nucleosil, 5-μm particle size, Phenomenex). Fractions were collected every minute and rotary evaporated to dryness. Fractions were treated with PNGase F, and an aliquot from each fraction was subjected to carbohydrate analysis using FACE. Fractions were stored at −4°C until LC/ESI-MS/MS analysis.

Liquid Chromatography/Electrospray Ionization (LC/ESI)-Tandem Mass Spectrometry (MS/MS) Analysis

A fraction from ZPC Lys-C digest was separated using a capillary C18 column (150 × 0.18 mm; Nucleosil, 5-μm particle size) and analyzed on a Finnigan LCQ ion trap mass spectrometer (San Jose, CA) with a modified electrospray ionization (ESI) source. A detailed scheme of the experimental setup for the LC/ESI-MS/MS analyses is described elsewhere [23]. Briefly, a positive voltage of 3 kV was applied to the electrospray needle, and a N_2 sheath flow (65 scale) was applied to stabilize the ESI signal. The LC/MS analysis was conducted using a Hewlett-Packard 1050 HPLC system (Palo Alto, CA) coupled to the LCQ. The mobile phase was split before the injector by a Tee-connector, and a flow rate of 2 μl/min was established through the capillary C18 column. The enzymatically digested peptides were eluted from the column using 0.5% formic acid in water (mobile phase A) and 0.5% formic acid in acetonitrile (mobile phase B) with a three-step linear gradient of 5% to 10% B in the first 10 min, 10% to 35% B in the next 40 min, and 35% to 40% B in the last 5 min. The LC/ESI-MS/MS analysis was accomplished using an automated data acquisition procedure in which a cyclic series of three different scan modes were performed. Data acquisition was conducted using the full scan mode (*m/z* 300–2000) to obtain the most intense peak (signal $>1.5 \times 10^5$ counts) as the precursor ion, followed by a high-resolution-zoom scan mode to determine the charge state of the precursor ion and an MS/MS scan mode (with a relative collision energy of 38%) to determine the structural fragment ions of the precursor ion. The resulting MS/MS spectra were then searched against a protein database (Owl) by Sequest to confirm the sequence of tryptic or chymotryptic peptides.

Sperm Binding Assay

The *N*-linked oligosaccharides of the VE, VE*, or fetuin were released with PNGase F and passed through a P2 column (Bio-Rad). Fractions containing oligosaccharides were identified using FACE analysis. The oligosaccharides were then passed through a C18 cartridge (Sigma), washed with 1 ml of water, and eluted with 100% methanol. FACE analysis confirmed that the eluted fraction contained predominantly complex-type oligosaccharides, while the wash fraction contained high-mannose oligosaccharides. The complex oligosaccharides were labeled with biotinylated-diaminopyridine (BAP; Pierce, Rockford, IL) by adding 10 μl of a BAP solution (25 mg/ml in DMSO) and 10 μl of 1-M cyanoborohydride. The reaction was incubated at 37°C for 24 h and passed through a TSK-3000

column to remove unreacted BAP regents. Fractions containing BAP-oligosaccharides were detected by monitoring fluorescence (excitation at 345 nm/emission at 400 nm). BAP-oligosaccharides were incubated with streptavidin-coated beads (5-μm diameter; Bangs Laboratories, Inc., Fishers, IN) under saturating conditions for 24 h. BAP-oligosaccharide-bound beads (~5.6×10^7 microspheres) were washed three times with 0.33 DB, resuspended in 200 μl of 0.33 DB, and stored at 4°C until use.

A sperm solution at a concentration of 6×10^5/ml in 0.33 DB was prepared as previously described. BAP-oligosaccharide-bound bead solution, 10 μl, was added to 90 μl of sperm in a microtiter plate and allowed to incubate for 5 min at room temperature. Sperm bound to beads were fixed with 4% glutaraldehyde in 0.33 DB. The number of sperm bound to 100 beads was determined with a microscope at 400× magnification. The assay was repeated three times.

RESULTS

N-Linked Carbohydrate Analysis of VE

The PNGase F-released and ANTS-derivatized *N*-linked oligosaccharides of the VE were analyzed by FACE. The VE glycoproteins possessed a microheterogeneous mixture of *N*-linked oligosaccharides (Fig. 1). Comparison of the almost identical profiles from the entire VE and isolated ZPC suggested that the majority of these oligosaccharides were derived from ZPC. Taking into account the percent composition of the VE glycoproteins (with the exclusion of ZPB since it lacks consensus *N*-linked sites), at least 71% of oligosaccharide profile of the VE was derived from ZPC. The *N*-linked profile of the activated egg envelope (VE*) showed an almost identical oligosaccharide pattern when compared to the VE and ZPC. Since these *N*-linked oligosaccharides migrated in the range of 5.8–16 degrees of polymerization with respect to a standard of linear glucose polymers, their composition was estimated to range from approximately 7–20 monosaccharide residues (Table 1). The oligosaccharides of the VE and ZPC were designated OS1, OS2, OS3, OS4, OS5, OS6, OS7, OS8, and OS9 as depicted in Figure 1.

Since Endo F1 digestion of glycoproteins releases only high-mannose and hybrid-type oligosaccharides, the presence of high-mannose or hybrid-type oligosaccharides was observed on digestion of the VE with Endo F1 (Fig. 2). The difference in the oligosaccharide patterns from the Endo F1 and PNGase F digestions is due to one less GlcNAc residue at the reducing ends of Endo F1-cleaved oligosaccharides. Comparison of the VE *N*-linked profiles before and after digestion with α-mannosidase confirmed that OS5, OS6, OS7, and OS8 were high-mannose-type oligosaccharides. Additionally, matrix-assisted laser desorption/ionization mass spectrometry analysis of the *N*-linked VE oligosaccharides also provided evidence for the presence of high-mannose glycans (Table 2).

The unaltered migration patterns of OS1, OS2, OS3, and OS4 in the *N*-linked profile after α-mannosidase treatment suggested that these slow migrating bands were complex-type oligosaccharides (Fig. 2). The absence of these bands from the Endo F1-treated VE sample (Fig. 2) provided additional evidence that OS1, OS2, OS3, and OS4 were complex-type oligosaccharides. Migration shifts in OS1, OS2, OS3, and OS4, which resulted from the digestion of the entire *N*-linked VE profile with β-*N*-acetylglucosaminidase, α-fucosidase, or α-galactosidase but not α-neuraminidase, also confirmed that these oligosaccharide species were neutral complex-type oligosaccharides (data not shown). Thus, the *N*-linked oligosaccharides of the VE are composed of a heterogeneous mixture of neutral complex and high-mannose-type oligosaccharides.

*Characterization of N-Linked Oligosaccharides of ZPC and ZPC**

To gain compositional information on the ZPC oligosaccharides, oligosaccharide bands derived from PNGase F-treated ZPC were extracted from FACE prep gels [24]. Oligosaccharides from ZPC* (isolated from VE*) were also isolated and sequenced to determine if the exo-glycosidases released in the cortical granule reaction altered the composition of the envelope glycoproteins. After elution from the gel slices, the isolated oligosaccharides were passed through a TSK-3000 gel filtration column before being treated with various exo-glycosidases. The exo-glycosidases used to sequence the oligosaccharides included bovine kidney β-*N*-acetylhexosaminidase (which cleaves both GlcNAc and galactose *N*-acetylgalactosamine [GalNAc] residues), *Diplococcus pneumoniae* β-*N*-acetylglucosaminidase (which has a specificity for only GlcNAc residues), α-fucosidase, α-galactosidase, β-galactosidase, and α-mannosidase. Degrees of polymerization positions relative to a standard glucose ladder were used to analyze the oligosaccharide structures [24].

OS5, OS6, OS7, and OS8 from ZPC were not digested by any of the exo-glycosidases except α-mannosidase. Comparison of the migration patterns of α-mannosidase-treated and untreated oligosaccharides identified high-mannose structures. The changes in the degrees of polymerization after mannose removal indicated that OS5, OS6, OS7, and OS8 were oligomannose 9, 8, 7, and 6, respectively (data not shown).

Sequencing of OS1 identified at least two different oligosaccharides comigrating with the same electrophoretic mobility (Fig. 3A). The major oligosaccharide species contained terminal α-Gal and α-Fuc residues. The minor oligosaccharide species contained terminal α-Gal and terminal β-GalNAc residues. Both species lacked terminal GlcNAc residues since OS1 was not digested by *D. pneumoniae* β-*N*-acetylglucosaminidase (Fig. 3, lane 3). Sequencing of OS1* from ZPC* revealed identical migration patterns as

TABLE 1. Degree of polymerization (DP) and mole percent of the *N*-linked oligosaccharides of the vitelline envelope.

	DP	Molar %
OS1	16.0	13.7
OS2	12.0	2.8
OS3	11.2	13.7
OS4	10.7	14.1
OS5	8.4	9.5
OS6	8.1	9.6
OS7	7.4	17.2
OS8	6.5	16.0
OS9	5.8	3.3

TABLE 2. Monosaccharide composition derived from MALDI masses of vitelline envelope oligosaccharides.

	Hexose	Fucose	HexNAc[a]	*m/z*
OS4a	6	3	5	2443.9
OS4b	6	3	5	2443.9
OS4c	5	3	6	2484.93
OS5	9	0	2	1882.64
OS6	8	0	2	1720.59
OS7	7	0	2	1558.54
OS8	6	0	2	1396.49
OS9	5	0	2	1234.46

[a] Hexose *N*-acetylhexosamine.

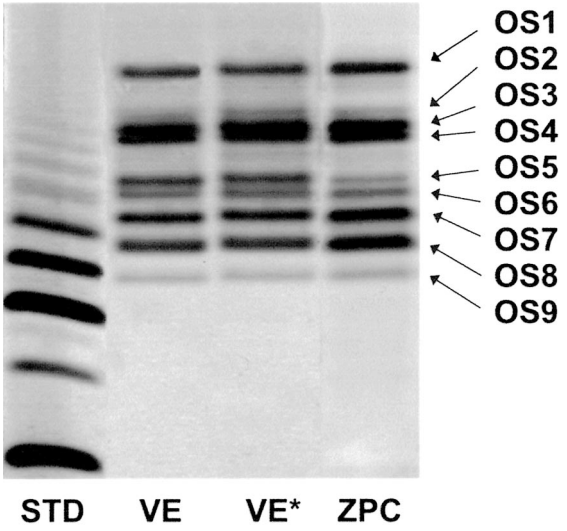

FIG. 1. The *N*-linked oligosaccharides from VE, VE*, and ZPC. ANTS-labeled *N*-linked oligosaccharides of the VE, VE*, and ZPC were resolved on a polyacrylamide gel. The STD lane refers to a linear glucose polymer ladder with G3 (glucose trimer) shown as the fastest-migrating band. Each band above G3 represents the successive increase of one glucose residue. Oligosaccharide bands were designated OS1–9.

OS1 (data not shown). This suggested that OS1 oligosaccharide was not a substrate for cortical granule glycosidases.

Analysis of OS2 digestion patterns showed that at least two oligosaccharide species were present (Fig. 3B). The major species possessed terminal α-Gal and α-Fuc residues. The minor species consisted of terminal β-GalNAc and α-Fuc residues. Since the OS2 and OS2* digestion patterns were identical (data not shown), OS2 oligosaccharide species were not substrates for cortical granule glycosidases.

Carbohydrate analysis of OS3 revealed that the oligosaccharide band consisted of at least two comigrating species (Fig. 3C). The major oligosaccharide species contained terminal α-Gal and α-Fuc residues and one terminal β-

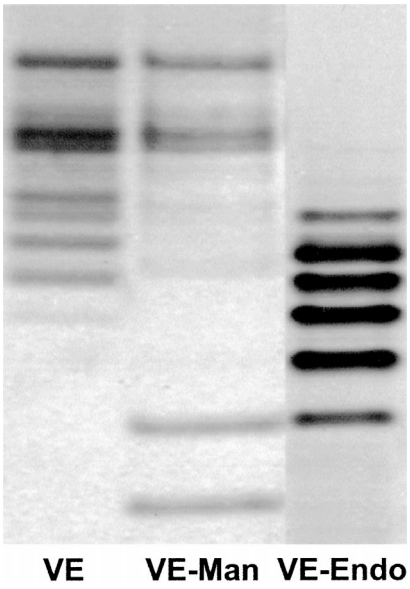

FIG. 2. High-mannose structures of the VE oligosaccharides. VE *N*-linked oligosaccharides were released/digested by PNGase F (VE), PNGase F and α-mannosidase (VE-Man), and Endo F1 (VE-Endo) and separated by polyacrylamide gel electrophoresis.

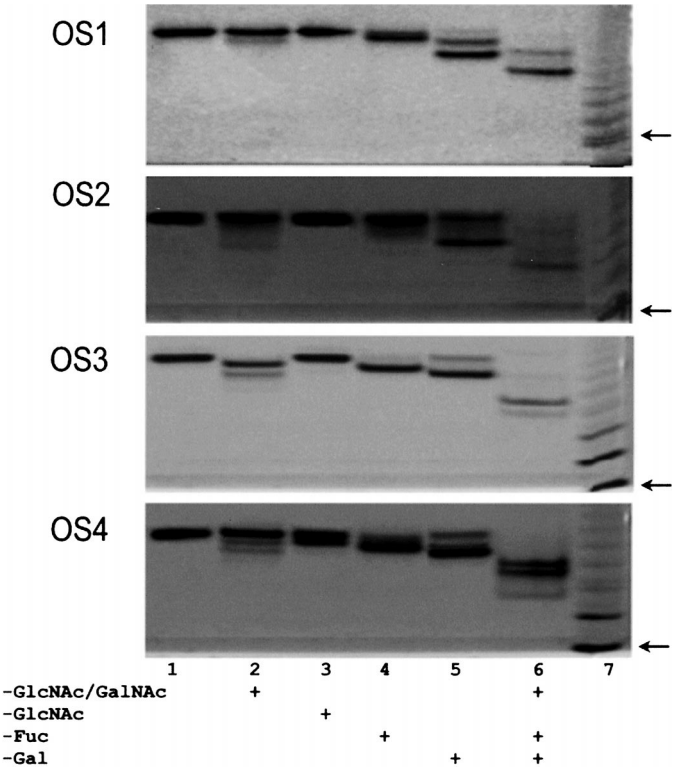

FIG. 3. Sequencing of the VE *N*-linked oligosaccharides, OS1, OS2, OS3, and OS4. Individual VE oligosaccharide bands were extracted from a polyacrylamide gel and treated with various exo-glycosidases. Gels A, B, C, and D are the hydrolysis products from OS1, OS2, OS3, and OS4, respectively. Lane 1: untreated oligosaccharide; lane 2: bovine kidney β-*N*-acetylhexosaminidase-treated oligosaccharide; lane 3: *D. pneumoniae* β-*N*-acetylglucosaminidase-treated oligosaccharide; lane 4: α-fucosidase-treated oligosaccharide; lane 5: α-galactosidase-treated oligosaccharide; lane 6: bovine kidney β-*N*-acetylhexosaminidase-, α-fucosidase-, α-galactosidase-, and β-galactosidase-treated oligosaccharide. Lane 7 is the glucose polymer ladder with the fastest-migrating bands as G8 for gel A, G8 for gel B, G5 for gel C, and G6 for gel D (arrows).

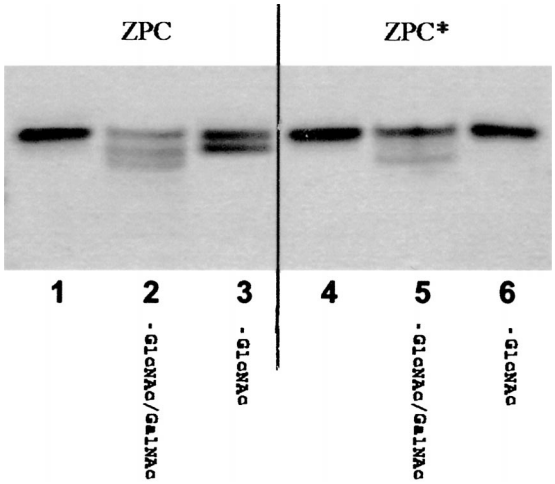

FIG. 4. Comparison of β-*N*-acetylglucosaminidase digestion patterns for *N*-linked oligosaccharides of ZPC and ZPC* OS4. The ZPC OS4 and the ZPC* OS4* bands were treated with bovine kidney β-*N*-acetylhexosaminidase and *D. pneumoniae* β-*N*-acetylglucosaminidase. Lanes 1, 2, and 3 are untreated OS4, OS4 hydrolyzed with bovine kidney β-*N*-acetylhexosaminidase, and OS4 with *D. pneumoniae* β-*N*-acetylglucosaminidase, respectively. Lanes 4, 5, and 6 are untreated OS4*, OS4* hydrolyzed with bovine kidney β-*N*-acetylhexosaminidase, and OS4* with *D. pneumoniae* β-*N*-acetylglucosaminidase, respectively.

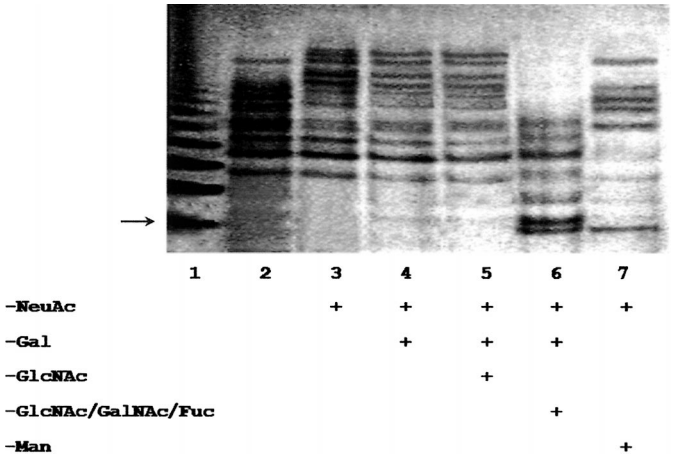

FIG. 5. Sequencing of the ZPA *N*-linked oligosaccharides. The *N*-linked oligosaccharides of ZPA were treated with a battery of exo-glycosidases. Lanes 1 and 2 represent a glucose polymer ladder (with G4 as the fastest-migrating band as shown by the arrow) and the untreated ZPA profile, respectively. The gel lanes correspond to the ZPA glycans digested with lane 3: α-neuraminidase; lane 4: α-neuraminidase, α-galactosidase, and β-galactosidase; lane 5: α-neuraminidase, α-galactosidase, β-galactosidase, and *D. pneumoniae* β-*N*-acetylglucosaminidase; lane 6: α-neuraminidase, α-galactosidase, β-galactosidase, bovine kidney β-*N*-acetylhexosaminidase, and α-fucosidase; and lane 7: α-neuraminidase and α-mannosidase.

GalNAc residue. The minor oligosaccharide species in the OS3 band contained terminal β-GalNAc and α-Fuc residues. Sequencing of OS3* showed identical digestion patterns as OS3 and suggested that OS3 was unaffected by cortical granule glycosidases (data not shown).

Analysis of the OS4 band revealed at least three comigrating oligosaccharide species (Fig. 3D). OS4 consisted of two dominant carbohydrate species and one minor component (designated OS4a, OS4b, and OS4c, respectively). OS4a possessed one terminal β-GlcNAc residue, one terminal α-Gal residue, and α-Fuc residues. OS4b was predicted to possess one terminal β-GalNAc residue, one terminal α-Gal residue, and α-Fuc residues. OS4c was predicted to possess terminal β-GalNAc and α-Fuc residues.

Of all the oligosaccharide species analyzed, only OS4 was digested by *D. pneumoniae* β-*N*-acetylglucosaminidase. Thus, a terminal GlcNAc residue in OS4a is a potential substrate for the cortical granule β-*N*-acetylglucosaminidase released by the cortical granule reaction. Interestingly, the same oligosaccharide species (OS4*) isolated from ZPC* of activated eggs possessed a different digestion pattern when treated with *D. pneumoniae* β-*N*-acetylglucosaminidase and bovine kidney β-*N*-acetylhexosaminidase (Fig. 4). OS4* was not digested by *D. pneumoniae* β-*N*-acetylglucosaminidase (inferring that terminal GlcNAc residues were absent); also, a band shift was not observed with the bovine kidney β-*N*-acetylhexosaminidase digestion.

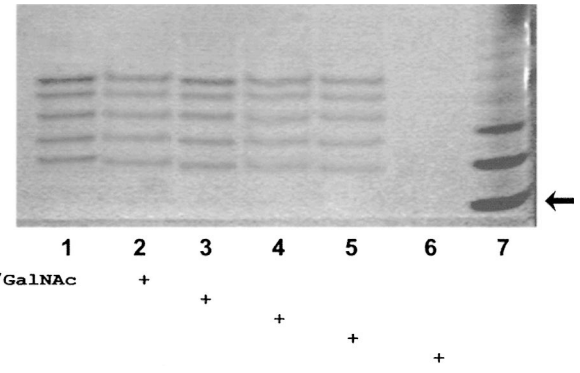

FIG. 6. Sequencing of the *N*-linked ZPX oligosaccharides. The *N*-linked ZPX glycans were digested with various exo-glycosidases. Lane 1: untreated; lane 2: bovine kidney β-*N*-acetylhexosaminidase; lane 3: *D. pneumoniae* β-*N*-acetylglucosaminidase; lane 4: α-fucosidase; lane 5: α-galactosidase and β-galactosidase; lane 6: α-mannosidase; lane 7: glucose polymer ladder with G5 as the fastest-migrating band as shown by the arrow.

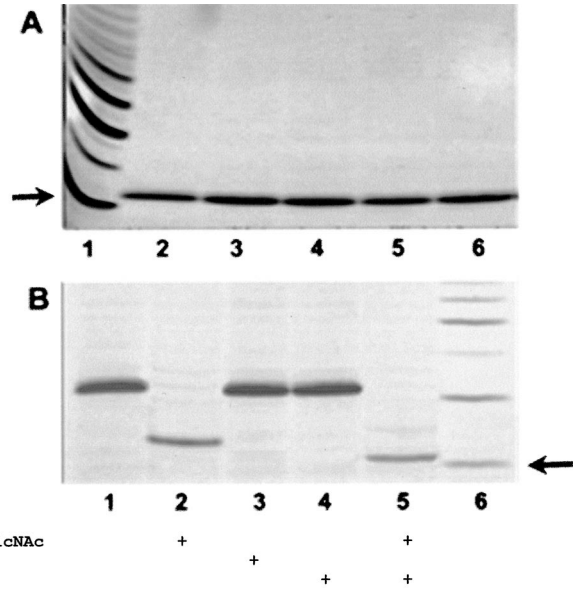

FIG. 7. Electrophoretic separation of the *O*-linked oligosaccharides from VE, VE*, ZPB, ZPC, and ZPC* and sequencing of the *O*-linked oligosaccharides of ZPC. The *O*-linked oligosaccharides of the VE, VE*, ZPB, ZPC, and ZPC* were released by hydrazinolysis and separated on a FACE *O*-linked polyacrylamide gel. **A**) Lane 1: glucose polymer ladder with G3 as the fastest-migrating band as shown by the arrow; lane 2: VE; lane 3: VE*; lane 4: ZPB; lane 5: ZPC; lane 6: ZPC*. The ZPC *O*-linked oligosaccharide was sequenced using various exo-glycosidases. **B**) Lane 1: untreated; lane 2: bovine kidney β-*N*-acetylhexosaminidase, lane 3: *D. pneumoniae* β-*N*-acetylglucosaminidase; lane 4: β-galactosidase; lane 5: bovine kidney β-*N*-acetylhexosaminidase and β-galactosidase; lane 6: glucose polymer ladder with G2 as the fastest-migrating band as shown by the arrow.

N-*Linked Analysis of ZPA and ZPX*

FACE analysis of ZPA revealed a heterogeneous mixture of glycans that was different from the VE/ZPC *N*-linked profile. Lane 7 of Figure 5 shows that high-mannose structures were present on ZPA since some of the oligosaccharide bands were shifted following α-mannosidase treatment. The upward shift of bands following α-neuraminidase treatment demonstrated that the complex-type oligosaccharides of ZPA possessed terminal sialic acid residues (Fig. 5, lane 3). Lane 6 of Figure 5 revealed that these acidic complex ZPA oligosaccharides, but not the high-mannose ZPA oligosaccharides, could be further digested with a mixture of α-neuraminidase, α-galactosidase, β-galactosidase, bovine kidney β-*N*-acetylhexosaminidase, and α-fucosidase. Treatment of the ZPA oligosaccharides individually (without the pretreatment with α-neuraminidase) with α-galactosidase, β-galactosidase, α-fucosidase, bovine kidney *N*-acetylhexosaminidase, or *D. pneumoniae* β-*N*-acetylglucosaminidase produced no band shifts, suggesting that none of the sub-

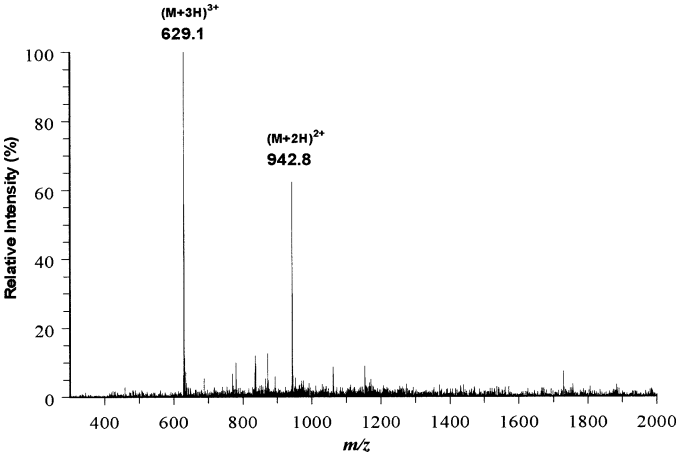

FIG. 8. Full scan MS spectrum of a ZPC peptide. A peptide containing N^{113} (amino acids 102–117, VLIQCFYPRNGNVSSK) was detected as a doubly charged ion at *m/z* = 942.8 and triply charged ion at *m/z* = 629.1.

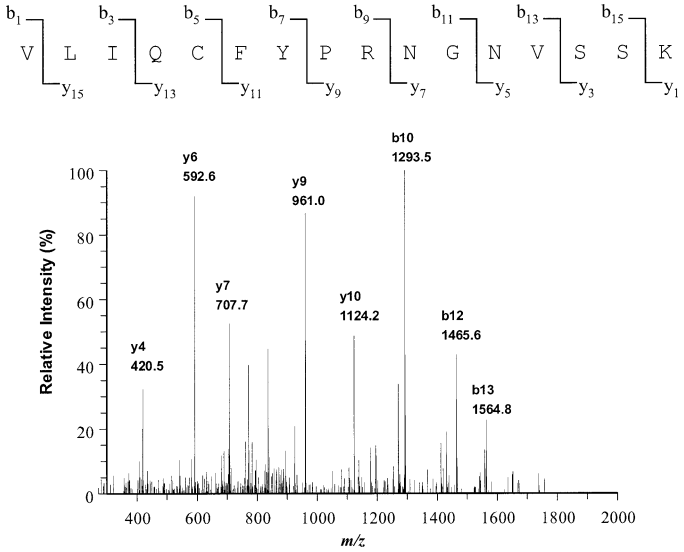

FIG. 9. The MS/MS spectrum of the ZPC peptide. MS/MS analysis of the peptide confirmed the peptide sequence (as corresponding to amino acids 102–117). The dominant ion products from the N-terminal fragments were y_4, y_6, y_7, y_9, and y_{10}. The dominant ion products from the C-terminal fragments were b_{10}, b_{12}, and b_{13}.

strates of these glycosidases were terminal monosaccharides of the ZPA glycans (data not shown).

When the *N*-linked ZPX oligosaccharides were analyzed with FACE, the majority of these glycans consisted of high-mannose structures (Fig. 6). The oligosaccharide bands from ZPX were resistant to all exo-glycosidases except α-mannosidase. Thus, similar to the ZPC high-mannose glycans, ZPX possessed oligomannose 9, 8, 7, 6, and 5 structures.

O-Linked Analysis of the VE, ZPB, and ZPC

O-linked oligosaccharides of VE, VE*, ZPB, ZPC, and ZPC* were released with hydrazinolysis. Hydrazinolysis at 60°C allowed the selective release of *O*-linked oligosaccharides [25]. The released oligosaccharides were re-*N*-acetylated and labeled with ANTS for FACE analysis. The VE, VE*, ZPB, ZPC, and ZPC* all exhibited the same *O*-linked oligosaccharide profile (Fig. 7A). The major oligosaccharide species from each lane in Figure 7A migrated in the same position as a trisaccharide (glucose trimer) in the oligosaccharide standard. Sequencing this *O*-linked glycan from ZPC revealed that the trisaccharide was not digestible when α-neuraminidase, α-galactosidase, α-fucosidase (data not shown), *D. pneumoniae* β-*N*-acetylglucosaminidase, and β-galactosidase were used singularly and in combination (Fig. 7B). Since the nonreducing end of the trisaccharide was only hydrolyzed with bovine kidney β-*N*-acetylhexosaminidase (lane 3), the terminal monosaccharide residue was deduced to be β-GalNAc. Only a combination of β-*N*-acetylhexosaminidase and β-galactosidase resulted in a second band shift (lane 5). Sequencing of the VE, VE*, and ZPB *O*-linked oligosaccharides showed the same digestion patterns (data not shown). Thus, the sequencing of the *O*-linked trisaccharide determined the structure to be GalNAc-β-Gal-β-GalNAc.

Glycosylation Mapping of ZPC

To map the *N*-linked glycosylation sites of ZPC, glycopeptides from an endoproteinase Lys-C digestion were separated by HPLC on a C18 column. FACE analysis was performed on the isolated glycopeptides to determine whether they possessed high-mannose or complex-type oligosaccharides. The subsequently deglycosylated peptides were analyzed by liquid chromatography/electrospray ionization-tandem mass spectrometry. When a fraction of the ZPC digest that contained solely high mannose oligosaccharides was analyzed by LC/ESI-MS/MS, a peptide that contained an *N*-linked consensus sequence (N^{113}) was detected. The peptide contained an Asp residue in place of the expected Asn residue as a result of the PNGase F digestion. Figure 8 shows the full scan mass spectrum of the N^{113}-containing peptide (amino acids 102–117), which was detected as both a doubly charged ion at *m/z* = 942.8 and triply charged ion at *m/z* = 629.1. These ions had masses that corresponded to the predicted 1855.3 Da for the amino acids 102–117 peptide with N→D conversion. To confirm the identity of the peptide, MS/MS analysis (Fig. 9) of the doubly charged ion at *m/z* = 942.8 was carried out. The MS/MS spectrum showed that the dominant product ions were generated from N-terminal fragments, y_n (n = 4, 6, 7, and 9–11) and C-terminal fragments, b_n (n = 7, 10, 12, and 13). These ions unambiguously confirmed that the peptide corresponded to amino acids 10–117 of the ZPC sequence with the Asn replaced with Asp.

We were unable to detect the peptide (amino acids 36–101) containing the other *N*-linked glycosylation site (N^{82}) in a Lys-C digestion fraction that contained solely complex-type oligosaccharides. LC/ESI-MS/MS analyses of other peptide fractions containing only complex-type oligosaccharides derived from other proteolytic digests (trypsin, chymotrypsin, and V8 protease) were unsuccessful. The inability to detect peptide fragments containing N^{82} may be due to the presence of *O*-linked oligosaccharides in the proximity of N^{82}. Since the ratio of the molar percent of complex to high-mannose oligosaccharides for ZPC was 1:1, we suggest that N^{82} was glycosylated with complex-type oligosaccharides and N^{113} with high-mannose oligosaccharides.

Sperm Binding Assay to Bead-Conjugated VE Oligosaccharides

To assess whether the PNGase F-released VE oligosaccharides alone could act as ligands for sperm binding with-

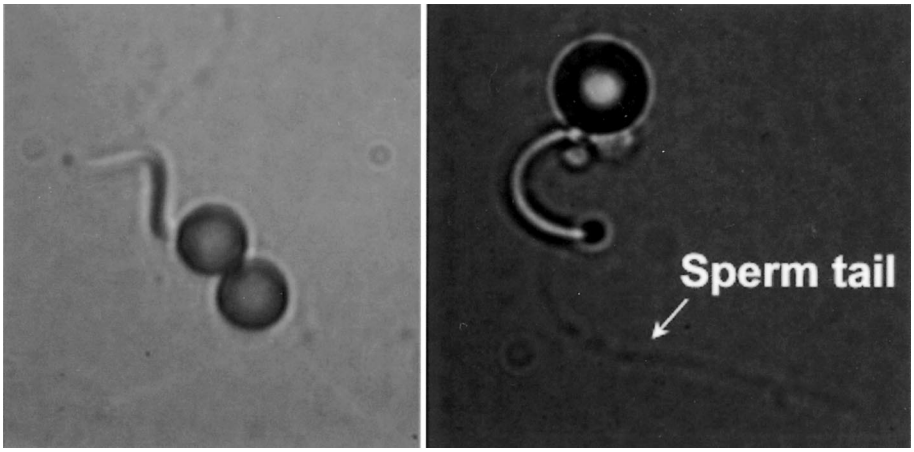

FIG. 10. Light micrographs of sperm bound to glycosylated beads. Magnification ×400.

out the polypeptide backbone of the VE glycoproteins, a sperm binding assay was developed that used biotinylated complex oligosaccharides of the VE attached to streptavidin-coated beads. We also assayed the ligand activity of the VE* complex oligosaccharides and fetuin glycans as controls. The number of sperm bound per 100 beads containing oligosaccharides of the VE, VE*, and fetuin were 35 ± 6, 10 ± 2.5, and 11 ± 3.6 (±SD, n = 3), respectively. Thus, VE oligosaccharides alone permitted specific sperm binding. Additionally, the loss of ligand activity in the VE* oligosaccharides provided additional evidence that the VE glycans were modified during the cortical granule reaction. The majority of the sperm bound the beads at the anterior portion of their heads (Fig. 10), which suggested the plasma membrane receptor was located over the sperm acrosome.

DISCUSSION

This report provides the first characterization of the *Xenopus* VE glycans and relates glycan structure to sperm binding function. The majority of the VE *N*-linked glycans were composed of a heterogeneous mixture of high-mannose and complex oligosaccharides derived from ZPC. The neutral *N*-linked complex oligosaccharides of ZPC possessed a range of terminal monosaccharides that included β-GlcNAc, β-GalNAc, α-Gal, and/or α-Fuc, while the high-mannose oligosaccharides included structures of oligo-mannose

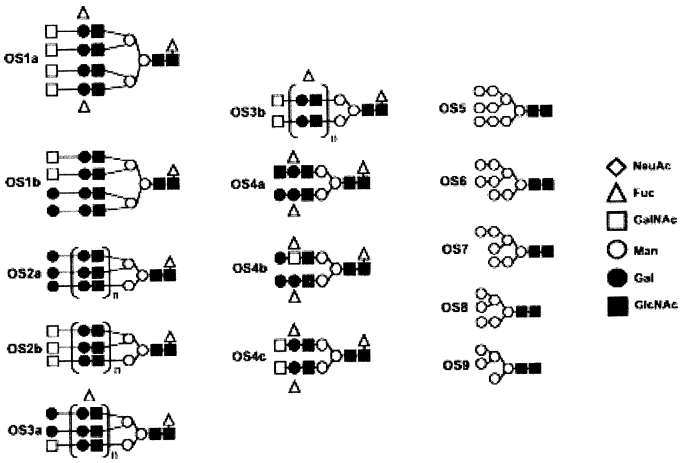

FIG. 11. Proposed structures for the *N*-linked VE oligosaccharides. All terminal Gal and Fuc residues are in the α anomeric configuration. All GlcNAc and GalNAc residues are in the β configuration. The number of repeating units is represented by n = 1 or 2.

9 through 5. ZPA also possessed a combination of complex and high-mannose oligosaccharides. However, the complex glycans of ZPA were acidic because of the presence of *N*-acetylneuraminic acid residues on their nonreducing ends. In contrast, ZPX only contained high-mannose oligosaccharides.

Complete digestion of the ZPC complex-type oligosaccharides to their trimannosyl core was not possible with the battery of sequencing exo-glycosidases used in this study. We were only able to obtain data on the terminal monosaccharide residues of each of these oligosaccharide species. Thus, complete structures for OS1, OS2, and OS3 could not be determined with the methods used here. One explanation for the ineffectiveness of the exo-glycosidases is the possible modification of the internal monosaccharides of ZPC glycans. However, we were able to obtain MALDI-MS data that corresponded to OS4a, OS4b, and OS4c (Table 2). Examination of the monosaccharide compositions of these oligosaccharides modification that blocked the sequencing reactions did not involve sulfation or phosphorylation. Based on knowledge of the general structural features of *N*-linked oligosaccharides, the predetermined migration patterns of oligosaccharides of known sequence [24], the migration patterns of the VE oligosaccharides resulting from digests with exo-glycosidaes, and MALDI-MS data, we predict that the VE oligosaccharides possess the structures displayed in Figure 11.

Terminal GlcNAc residues were present on the OS4 oligosaccharide of ZPC. The involvement of GlcNAc residues in *Xenopus* gamete interactions was first reported by Prody et al. [16]. Treatment of oviposited eggs with purified cortical granule β-*N*-acetylglucosaminidase or Jack bean β-*N*-acetylglucosaminidase rendered eggs unfertilizable. Additionally, we previously demonstrated that the removal of GlcNAc residues with *Xenopus* cortical granule β-*N*-acetylglucosaminidase and commercial β-*N*-acetylglucosaminidases resulted in the loss of VE ligand activity in a sperm binding assay [9]. GlcNAc residues have also been reported to play a role in mouse fertilization. Miller et al. [26] proposed that sperm-zona binding and activation of the acrosome reaction in the mouse were initiated by sperm β-1,4-galactosyltransferase binding to terminal GlcNAc residues from the *O*-linked oligosaccharides of ZPC. However, the role of sperm β-1,4-galactosyltransferase in the mouse has been recently refined to emphasize its role in signal transduction to induce the acrosome reaction [27]. Consistent with the results presented here, the presence of terminal

GlcNAc residues has been reported in both mouse and porcine *N*-linked and *O*-linked oligosaccharides [28–31].

We demonstrated a difference between the oligosaccharide composition of ZPC and ZPC* that could account for the VE's loss of ligand activity after fertilization. We propose that removal of the terminal GlcNAc residue from OS4 by cortical granule β-*N*-acetylglucosaminidase is a mechanism to prevent polyspermy. The enzymatic activity of cortical granule β-*N*-acetylglucosaminidase released by the cortical granule reaction on the glycoproteins of the VE/zona as a mechanism to prevent polyspermy was proposed by Prody et al. [16] for *Xenopus* and more recently by Miller et al. [32] for the mouse. Oligosaccharide modifications of the mouse and rat zona based on changes in lectin affinities of the egg after fertilization have been reported [33, 34]. Additionally, oligosaccharide modifications have been reported in bovine zona glycoproteins, which showed a loss of sialic acid residues on fertilization [8].

The *Xenopus* VE *O*-linked oligosaccharide is a trisaccharide with the structure GalNAc-β-Gal-β-GalNAc. We previously reported that the *O*-linked oligosaccharides of the VE were not involved in sperm-VE binding. Since *Xenopus* sperm-VE binding is dependent on GlcNAc and Fuc residues [9], the lack of these critical residues on the *O*-linked oligosaccharides of the VE support the sole involvement of *N*-linked oligosaccharides in the ligand activity of the VE. Interestingly, Nagdas et al. [29] reported the presence of an *O*-linked trisaccharide on mouse ZPC with a related structure, GlcNAc-β-Gal-β-GalNAc. Their analysis suggested that this *O*-linked trisaccharide is the only *O*-linked glycan present on mouse ZPA and ZPC. However, since the Nagdas et al. results were obtained using Jack bean β-*N*-acetylglucosaminidase (with a substrate specificity for both GlcNAc and GalNAc residues), another possible structure for the *O*-linked trisaccharide on the mouse ZPC would be GalNAc-β-Gal-β-GalNAc (the same structure we propose here for the *Xenopus O*-linked oligosaccharides). Contrasting the Nagdas et al. analysis on the mouse *O*-linked oligosaccharides are the results of Easton et al. [31], who used mass spectrometry to characterize glycan structures. Easton et al. reported that the majority of the *O*-linked oligosaccharides from mouse zona were core 2 structures (Galβ1-4GlcNAcβ1-6[Galβ1-3]GalNAc) terminated with one or two *N*-acetyl or *N*-glycolylneuraminic acid residues. Differences in the results of these two studies are not easily explained since both groups employed β-elimination to release the *O*-linked oligosaccharides. One possibility is differences in sample preparation: Nagdas et al. isolated zona components from the eggs of superovulated mice, while Easton et al. isolated zona from an ovary homogenate. In this case, egg maturation state may affect the oligosaccharide structures present. Relevant to this suggestion is the paper of Aviles et al. [35], which reported differences in oligosaccharide composition of the mouse zona during folliculogenesis.

In a direct binding study, we demonstrated that the complex oligosaccharide moieties of the VE alone were sufficient to support sperm binding. Thus, the polypeptide moiety of ZPC glycoproteins may not be essential to sperm-VE binding. However, the polypeptide moiety may not be without function in sperm-VE binding. The polypeptide moiety may provide a structural framework for the attachment of glycans. This multivalency may affect the strength of sperm binding receptors to glycan ligands on the ZPC glycoproteins. Several studies have shown that the oligosaccharides released from the zona are capable of inhibiting sperm binding. The lack of ligand activity of the VE* oligosaccharides suggested that these glycans were modified. This observation supports the hypothesis that cortical granule β-*N*-acetylglucosaminidase activity is one of the mechanisms to prevent polyspermy. We also observed that sperm binding to glycosylated beads was also localized to the anterior portion of the sperm head. In combination with a previous report that amphibian sperm bind to the VE prior to undergoing the acrosome reaction [10], the receptors for sperm binding to the VE may be located on the plasma membrane directly exterior to the acrosome.

We determined that N^{113} of ZPC was glycosylated with only high-mannose oligosaccharides. This glycosylation site is evolutionarily conserved in all ZPC homologues [2]. Since high-mannose structures are the precursors in the glycosylation pathway to more diversified oligosaccharides, all cells are able to express these oligomannose glycans. Thus, the occupancy of a glycan at this conserved glycosylation site may be of fundamental and evolutionarily conserved importance to the three-dimensional structure of ZPC glycoproteins.

From the mapping of the glycosylation sites on the polypeptide of ZPC, we propose that sperm bind to the complex oligosaccharides located at N^{82} of ZPC. The glycan structure necessary for this interaction is OS4a, which is the only structure that possessed a terminal GlcNAc residue. Considering the microheterogeneous nature of ZPC complex oligosaccharides and our finding that only one of these glycan structures possessed a terminal GlcNAc residue, the question rises whether every ZPC molecule possesses ligand activity. Since mechanistic redundancy in several of the crucial steps in fertilization has been observed [27, 36], it is possible that other oligosaccharides of the VE also act as ligands for sperm binding. However, another explanation for the ability of only a single glycan structure to act as a ligand for sperm binding is alterations in ZPC glycosylation during egg maturation, whereby a majority of OS4a oligosaccharide may be located on the outer portion of the VE.

Because of the limitation in the quantity of zona oligosaccharides that can be obtained from mammalian species, determination of the molecular structures of ligands involved in sperm-egg envelope binding has not yet been possible. With the characterization of oligosaccharide structures from the *Xenopus* egg envelope reported here, synthetic oligosaccharides with defined structures can be used to investigate the initial sperm binding reaction in fertilization. Synthetic oligosaccharides that correspond to the structures found on the *Xenopus* VE glycoproteins can provide an approach for analyzing the functional roles of carbohydrates in species-specific fertilization, induction of the acrosome, and the prevention of polyspermy.

ACKNOWLEDGMENTS

We thank Paul Tu, Tina Lu, and Ruben Almarez for their technical assistance and Dr. LeAnn Lindsay for insightful discussions. We appreciate the assistance from Drs. Carlito Lebrilla and Ken Tseng for MALDI analysis. We also thank Dr. Chris Starr, Chuck Hague, and Irene Masada at Glyko, Inc., for their assistance in providing reagents, useful discussions, and review of this manuscript.

REFERENCES

1. Harris JD, Hibler DW, Fontenot GK, Hsu KT, Yurewicz EC, Sacco AG. Cloning and characterization of zona pellucida genes and cDNAs from a variety of mammalian species: the ZPA, ZPB and ZPC gene families. DNA Seq 1994; 4:361–393.

2. Hedrick JL. Comparative structural and antigenic properties of zona pellucida glycoproteins. J Reprod Fertil Suppl 1996; 50:9–17.
3. Florman HM, Wassarman PM. *O*-linked oligosaccharides of mouse egg ZP3 account for its sperm receptor activity. Cell 1985; 41:313–324.
4. Litscher ES, Wassarman PM. Characterization of mouse ZP3-derived glycopeptide, gp55, that exhibits sperm receptor and acrosome reaction-inducing activity in vitro. Biochemistry 1996; 35:3980–3985.
5. Yonezawa N, Mitsui S, Kudo K, Nakano M. Identification of an N-glycosylated region of pig zona pellucida glycoprotein ZPB that is involved in sperm binding. Eur J Biochem 1997; 248:86–92.
6. Yurewicz EC, Pack BA, Sacco AG. Isolation, composition, and biological activity of sugar chains of porcine oocyte zona pellucida 55K glycoproteins. Mol Reprod Dev 1991; 30:126–134.
7. Yurewicz EC, Sacco AG, Gupta SK, Xu N, Gage DA. Hetero-oligomerization-dependent binding of pig oocyte zona pellucida glycoproteins ZPB and ZPC to boar sperm membrane vesicles. J Biol Chem 1998; 273:7488–7494.
8. Katsumata T, Noguchi S, Yonezawa N, Tanokura M, Nakano M. Structural characterization of the *N*-linked carbohydrate chains of the zona pellucida glycoproteins from bovine ovarian and fertilized eggs. Eur J Biochem 1996; 240:448–453.
9. Vo LH, Hedrick JL. Independent and hetero-oligomeric-dependent sperm binding to egg envelope glycoprotein ZPC in *Xenopus laevis*. Biol Reprod 2000; 62:766–774.
10. Omata S, Katagiri C. Involvement of carbohydrate moieties of the toad egg vitelline coat in binding with fertilizing sperm. Dev Growth Differ 1996; 38:663–672.
11. Tian J, Gong H, Thomsen GH, Lennarz WJ. Gamete interactions in *Xenopus laevis*: identification of sperm binding glycoproteins in the egg vitelline envelope. J Cell Biol 1997; 136:1099–1108.
12. Hedrick JL, Nishihara T. Structure and function of the extracellular matrix of anuran eggs. Journal of Electron Mircoscopy Technique 1991; 17:319–335.
13. Lindsay LL, Wieduwilt MJ, Hedrick JL. Oviductin, the *Xenopus laevis* oviductal protease that process egg envelope glycoprotein gp43, increase sperm binding to envelopes, and is translated as part of an unusual mosaic protein composed of two protease and several CUB domains. Biol Reprod 1999; 60:989–995.
14. Lindsay LL, Hedrick JL. Proteases released from *Xenopus laevis* eggs at activation and their role in envelope conversion. Dev Biol 1989; 135:202–211.
15. Lindsay LL, Yang JC, Hedrick JL. Ovochymase, an *Xenopus laevis* egg extracellular protease, is translated as part of a polyprotein. Proc Natl Acad Sci U S A 1999; 96:11253–11258.
16. Prody GA, Greve LC, Hedrick JL. Purification and characterization of an N-acetyl-beta-D-glucosaminidase from cortical granules of *Xenopus laevis* eggs. J Exp Zool 1985; 235:335–340.
17. Tian J, Gong H, Lennarz WJ. *Xenopus laevis* sperm receptor gp69/64 glycoprotein is a homolog of the mammalian sperm receptor ZP2. Proc Nat Acad Sci U S A 1999; 96:829–834.
18. Yang JC, Hedrick JL. cDNA Cloning and sequence analysis of the *Xenopus laevis* egg envelope glycoprotein gp43 (ZPC). Dev Growth Differ 1997; 39:457–467.
19. Lindsay LL, Wallace MA, Hedrick JL. A Hatching enzyme substrate in the *Xenopus laevis* egg envelope is a high molecular weight ZPA homolog. Dev Growth Differ 2001; 43:305–313.
20. Takasaki S, Mori E, Mori T. Structures of sugar chains included in mammalian zona pellucida glycoproteins and their potential roles in sperm-egg interaction. Biochim Biophys Acta 1999; 1473:206–215.
21. Dell A, Morris HR, Easton RL, Patankar M, Clark GF. The glycobiology of gametes and fertilization. Biochim Biophys Acta 1999; 1473:196–205.
22. Hedrick JL, Hardy DM. Isolation of extracellular matrix structures from *Xenopus laevis* oocytes, eggs, and embryos. Methods Cell Biol 1991; 36:231–234.
23. Yen TY, Joshi RK, Yan H, Seto NOL, Palcic MM, Macher BA. Characterization of cysteine residues and disulfide bonds in proteins by liquid chromatography/electrospray ionization tandem mass spectrometry. J Mass Spectrom 2000; 35:990–1002.
24. Starr CM, Masada RI, Hague C, Skop E, Klock JC. Fluorophore-assisted carbohydrate electrophoresis in the separation, analysis, and sequencing of carbohydrates. J Chromatogr A 1996; 720:295–321.
25. Patel T, Bruce J, Merry A, Bigge C, Wormald M, Jaques A, Parekh R. Use of hydrazine to release in intact and unreduced form both N- and O-linked oligosaccharides from glycoproteins. Biochemistry 1993; 32:679–693.
26. Miller DJ, Macek MB, Shur BD. Complementarity between sperm surface beta-1,4-galactosyltransferase and egg-coat ZP3 mediates sperm-egg binding. Nature 1992; 357:589–593.
27. Lu Q, Shur BD. Sperm from beta 1,4-galactosyltransferase-null mice are refractory to ZP3-induced acrosome reactions and penetrate the zona pellucida poorly. Development 1997; 124:4121–4131.
28. Hirano T, Takasaki S, Hedrick JL, Wardrip NJ, Amano J, Kobata A. *O*-linked neutral sugar chains of porcine zona pellucida glycoproteins. Eur J Biochem 1993; 214:763–769.
29. Nagdas SK, Araki Y, Chayko CA, Orgebin-Crist MC, Tulsiani DR. O-linked trisaccharide and N-linked poly-N-acetyllactosaminyl glycans are present on mouse ZP2 and ZP3. Biol Reprod 1994; 51:262–272.
30. Yonezawa N, Fukui N, Kudo K, Nakano M. Localization of neutral N-linked carbohydrate chains in pig zona pellucida glycoprotein ZPC. Eur J Biochem 1999; 260:57–63.
31. Easton RL, Patankar MS, Lattanzio FA, Leaven TH, Morris HR, Clark GF, Dell A. Structural analysis of murine zona pellucida glycans: evidence for the expression of core 2-type O-glycans and the Sd(a) antigen. J Biol Chem 2000; 275:7731–7742.
32. Miller DJ, Gong X, Decker G, Shur BD. Egg cortical granule N-acetylglucosaminidase is required for the mouse zona block to polyspermy. J Cell Biol 1993; 123:1431–1440.
33. Aviles M, Jaber L, Castells MT, Ballesta J, Kan FW. Modifications of carbohydrate residues and ZP2 and ZP3 glycoproteins in the mouse zona pellucida after fertilization. Biol Reprod 1997; 57:1155–1163.
34. Raz T, Skutelsky E, Shalgi R. Post-fertilization changes in the zona pellucida glycoproteins of rat eggs. Histochem Cell Biol 1996; 106: 395–403.
35. Aviles M, El-Mestrah M, Jaber L, Castells MT, Ballesta J, Kan FW. Cytochemical demonstration of modification of carbohydrates in the mouse zona pellucida during folliculogenesis. Histochem Cell Biol 2000; 113:207–219.
36. Baba T, Azuma S, Kashiwabara S, Toyoda Y. Sperm from mice carrying a targeted mutation of the acrosin gene can penetrate the oocyte zona pellucida and effect fertilization. J Biol Chem 1994; 269:31845–31849.
37. Lindsay LL, Yang JC, Hedrick JL. Identification and characterization of a unique *Xenopus laevis* egg envelope component, ZPD. Dev Growth Differ 2002; 44:205–212.